Diagnostic and Interventional Imaging (2015) **96**, 1261—1278

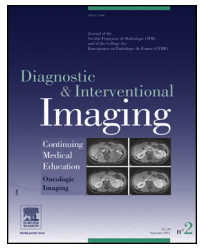

CONTINUING EDUCATION PROGRAM: FOCUS...

Entrapment and traumatic neuropathies of the elbow and hand: An imaging approach

A. Deniel[a,*], **A. Causeret**[a], **T. Moser**[b], **Y. Rolland**[c], **T. Dréano**[d], **R. Guillin**[a]

[a] *Department of Medical Imaging, Rennes University Hospitals, Sud Hospital, 16, boulevard de Bulgarie, 35203 Rennes cedex 2, France*
[b] *Department of Radiology, Montreal University Hospital Centre, 1560, rue Sherbrooke-Est, Montreal, Quebec H2 4M1, Canada*
[c] *Department of Medical Imaging, Eugène Marquis Centre, avenue de la Bataille-Flandres-Dunkerque, 35000 Rennes, France*
[d] *Department of Orthopaedics and Traumatology, Rennes University Hospitals, 2, rue Henri-Le-Guilloux, 35000 Rennes, France*

KEYWORDS
Ultrasound;
MRI;
Peripheral nerves;
Upper limb

Abstract Ultrasound and magnetic resonance imaging currently offer a detailed analysis of the peripheral nerves. Compressive and traumatic nerve injuries are the two main indications for imaging investigation of nerves with several publications describing the indications, technique and diagnostic capabilities of imaging signs. Investigation of entrapment neuropathies has three main goals, which are to confirm neuronal distress, search for the cause of nerve compression and exclude a differential diagnosis on the entire nerve. For traumatic nerve injuries, imaging, predominantly ultrasound, occasionally provides essential information for management including the type of nerve lesion, its exact site and local extension.

Upper limb nerves can be subjected to various injuries; the great majority of them involve compression and trauma. Apart from the median, ulnar and radial nerves, several less well-known motor and/or sensory nerves must not be disregarded. Whilst magnetic resonance imaging (MRI) can achieve these aims because of a high contrast resolution [1], ultrasound is the most commonly used tool in clinical practice because of its spatial resolution, accessibility and limited costs. The goal of this review was to describe the main points arising from the international literature about compressive and traumatic upper limb neuropathies before or after surgery.

* Corresponding author.
E-mail addresses: arnaud.deniel35@gmail.com, arnaud.deniel@chu-rennes.fr (A. Deniel).

http://dx.doi.org/10.1016/j.diii.2015.10.006

General details

Nerve anatomy

Peripheral nerves are made of many fascicles which themselves are made of numerous nerve fibers. Each nerve fiber is contained in a supporting tissue layer known as the endoneurium and each fascicle is surrounded by the perineurium, whereas the nerve is contained within a peripheral sheath known as the epineurium. The epineurium receives arterioles and venules, which provide neuronal vascularization [2].

Ultrasound appearance of peripheral nerves

The internal architecture of the nerve on ultrasound has a ''pseudo-ovular'' appearance. The fascicles are hypoechogenic surrounded by hyperechogenic epineural supporting tissue. This appearance differs from the more hyperechogenic, finely fibrillar and anisotropic appearance of tendons. The thickness of the nerve is influenced by gender [3—5] and possibly by weight [5] and patient age [3,4].

MRI anatomy of peripheral nerves

The signal of normal peripheral nerves is identical to that of adjacent muscles on T1- and T2-weighted MR images but may be slightly more intense on T2-weighted images [6,7]. Like the tendons, nerves are subjected to ''magic angle'' artifacts [8]. Because of the existence of the ''blood-nerve'' barrier, the normal nerve does not substantially enhance after intravenous administration of gadolinium chelate [6].

Entrapment neuropathies

Pathophysiology of nerve compression

Nerve compression results in a pathophysiological cascade in which microcirculatory disorders play a key role. It has been shown in animal models that nerve compression rapidly reduces the circulation in venules [9]. Prolonged compression results in ischemia, which itself causes blood vessel endothelial permeability abnormalities in the endoneurium, which are responsible for intrafascicular edema [10—12]. The resultant raised intrafascicular fluid pressure persists and maintains neuronal compression because of the blood-nerve barrier and the small number of lymph vessels within the endoneurium [2].

At an early stage of compression, neuronal ischemia results in axonal transport abnormalities, which cause only symptomatic reversible damage [2]. At a later stage, the epineural and endoneural interstitial edema is combined with structural changes in the nerve, initially involving damage to the myelin sheath (persistent or recurrent symptoms) and then later, axonal damage causing actual signs of denervation (sensory disorders and muscle wastage). Recovery of the nerve by axonal growth is then slow and occasionally incomplete at this stage. In the long term, peri- and endoneural edema is believed to activate fibroblast recruitment, leading to fibrosis of the supporting tissues [10].

Because the nerve is fixed as a result of the edema, the inhibition of gliding may induce stretching lesions which are also harmful [2]. In addition, proximal compression of the nerve renders it more liable to distal compression, and vice versa. This effect is known by the term of ''double crush syndrome'' [13], which should be considered if treatment fails at a given level.

Ultrasound appearance of nerve compression

Investigation of nerve canal symptoms has three purposes: to confirm nerve distress, investigate for an anatomical or extrinsic cause for the neuronal compression and to look for a differential diagnosis throughout the length of the nerve (particularly a neurogenic tumor).

The signs of compressive nerve distress consist of local thickening of the nerve, hypoechogenicity with loss of its fasciculated appearance and intra-neural hypervascularization in color or power Doppler (Fig. 1). Pathophysiologically, the hypoechogenicity and increased diameter of the nerve occur as a result of the edema developing in the endo- and perineural spaces (Fig. 2).

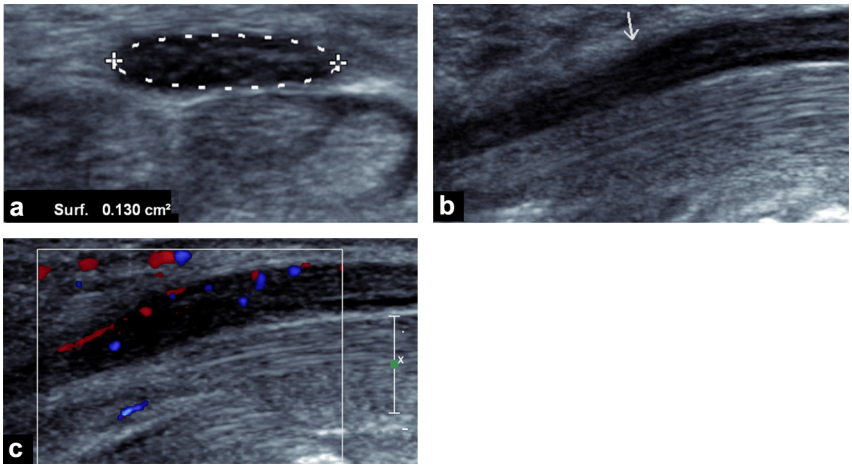

Figure 1. Ultrasound signs of nerve distress in a patient with carpal tunnel syndrome confirmed by electromyogram. a: cross-sectional area of the median nerve (dots) measuring 13 mm^2 with hypoechogenicity of the nerve; b: longitudinal section shows increased diameter proximal to the entrance to the carpal tunnel (arrow); c: Doppler ultrasound in color mode shows intra-neural hyperemia.

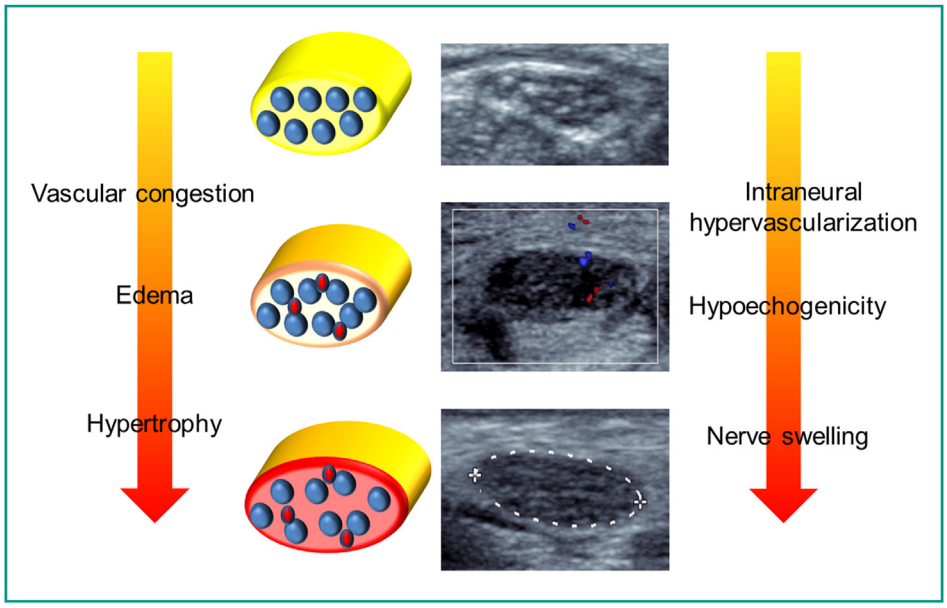

Figure 2. Pathophysiology and ultrasound signs of compressive nerve distress.

By consensus, nerve thickening is quantified by measuring the cross-sectional area (CSA). Measurement using a continuous trace is preferable to an elliptical ROI, defining the contour of the nerve from inside its peripheral hyperechogenic rim. This technique has been shown to offer good reproducibility for both the median and ulnar nerves [14—17]. The increase in diameter, often extending along the nerve, results in a characteristic imprint longitudinally when it passes beneath the compressive arcade.

Intra-neural hypervascularization is clearly visible on high-resolution ultrasound. Any intra-neural Doppler signal should be considered as an indicator of abnormal hypervascularization [17—19]. Power Doppler appears more effective than color Doppler to detect slow flow in the nerve [20].

Whilst direct visualization of compressive fibrous arcades is often considered to be difficult, investigation for an extrinsic compressive mass is the second key objective of ultrasound. This includes, for example, supernumerary muscles, arthrosynovial cysts and joint or tendon sheath tumors. Although the precise level of the lesion is often strongly suggested by electromyography, routine scanning of the nerve over its entire length using the ''lift'' technique should be used systematically in order to not miss a remote lesion such as a neurogenic tumour.

Finally, dynamic investigation of the nerve is a useful adjunct to static examination, because it may show reduced neuronal mobility as a result of compression (for example at the wrist) or abnormally increased mobility because of chronic instability (particularly at the elbow).

MRI appearance of nerve compression

Visualization of direct signs of nerved distress on MRI is inconstant [6,21—24]. An increased signal on T2-weighted images indicates neuronal edema although this feature is not specific because it can be observed in asymptomatic patients [6,7,25,26]. Conversely, a decrease in signal intensity on T2-weighted images occurs less commonly in neuronal fibrosis at an advanced stage [25]. Nerve enhancement is absent in the normal state and may be seen after intravenous administration of gadolinium chelate in nerve distress [6]. Morphological nerve changes may be visible although measurement of these is less satisfactory than with ultrasound because of poor spatial resolution and difficulties visualizing the nerve in its length.

In experimental nerve damage, signs of muscle denervation appear early (from 24 h) as a moderate rise in signal intensity on STIR images in the affected area [27]. This sign, which has limited sensitivity in chronic nerve compression, may be helpful when direct signs of nerve distress are absent [28], pending a knowledge of motor territories of the different upper limb nerves [29]. In advanced chronic damage, muscle atrophy and fatty changes are detected more easily than on ultrasound. MRI is only a second-line investigation in addition to ultrasound to look for signs of muscle denervation, to identify a compressive mass and in a postoperative context [30]. The investigation protocol is often limited to T1- and T2-weighted images with fat suppression in the transverse plane, combined with T1-weighted fat-suppressed images obtained after intravenous administration of gadolinium chelate in the transverse plane preoperatively for lesion characterization although these are used routinely postoperatively, particularly to search for small fibrous scars.

Median nerve at the wrist

Compression of the median nerve at the wrist known as the ''carpal tunnel syndrome'' (CTS), is the most common upper limb compressive neuropathy and occurs as a result of compression of the nerve beneath the flexor retinaculum. Although it is usually idiopathic, many causes are described, particularly including tumors and pseudomasses inside the canal, including tumors of the median nerve itself (schwannoma, fibrolipoma), tenosynovial hypertrophy and supernumerary muscles. The 2013 guidelines of the French

National Health Authority (HAS) indicate that carpal tunnel imaging is useless in case of typical clinical scenario but is indicated when unusual symptoms are present such as occurrence during an effort, a young age, a sudden onset, a suspected responsible underlying disease and in case of diagnostic uncertainty (negative EMG), or failure or recurrence after surgery [31].

Preoperative imaging

Ultrasound

Increased cross-sectional area (CSA) of the median nerve is recognized to be the best performing parameter, although there is no consensus about the cut-off value to be used, which ranges depending on the study between 9 and 15 mm^2 [14,15,17—19,32—44]. A cut-off of 11 mm^2 however appears to be often used (Table 1). A uniform cut-off value however may be questioned because of interindividual physiological variations [3—5]. Some authors have proposed standardizing the technique by incorporating the difference in nerve CSA measured in the canal tunnel and more proximally, 12 cm towards the elbow [45] or next to the pronator quadratus muscle, which is easier to perform [41]. Klauser et al. reported that a difference greater than 2 mm^2 results in a sensitivity of 99% and a specificity of 100% for the diagnosis of carpal tunnel syndrome [42]. Hunderfund et al. and Tajika et al. confirmed that this diagnostic method offers good diagnostic performance [43,44].

In the specific case of a bifid median nerve, the optimal threshold values are the same or slightly greater than those found without a bifid nerve. Using a threshold value of 11 mm^2 Bayrak et al. found a sensitivity of 90% and a specificity of 99% [46]. Using a threshold value of 12 mm^2 Klauser et al. found a sensitivity of 84.9% and a specificity of 46.5% (Fig. 3) [47]. Klauser et al. proposed using a delta CSA of 4 mm^2 in the forearm to improve the diagnostic performance of the measurement, yielding a sensitivity of 92.5% and a specificity of 94.6% [47].

Measurement of the CSA at the carpal tunnel outlet has also been discussed. Some authors consider this to be of limited value and difficult to perform [15,43,48], whereas others believe that it increases the sensitivity of the investigation [49,50]. In any event, ultrasound examination of the canal to its distal end is essential to detect isolated nerve distress at this level and to identify a deep occult compressive cause, such as a synovial palmar cyst (Fig. 4).

Intra-neural hyperemia is a useful sign for the diagnosis of nerve distress with sensitivity ranging from 41 to 95% and specificity from 71 to 100% [18,19,51—53]. These differences are probably due to variations in protocols, which limit its validity [20]. Overall, hypoechogenicity of the nerve with loss of fasciculated structure, although subjective, is a strong variable when combined with the above-mentioned signs. In addition to these three most classical signs of CTS, increased carpal tunnel pressure may result in palmar bulging of the flexor retinaculum. This is assessed by measuring the distance between the end point of the retinaculum and a virtual line traced between the apex of the trapezium tubercle and the hamulus of the hamate. A value of $\geq$ 2—4 mm is significantly associated with CTS [15,17,19,35]. The flattening index, which is the ratio of the greater to smaller diameter of the nerve, is pathological if it is over 3 [17,19,33,37]. These criteria, however, are not widely used in everyday practice.

Finally, dynamic flexion-extension of fingers can be used to assess transverse mobility of the median nerve beneath the flexor retinaculum and may be reduced in CTS [17,54,55]. This is assessed subjectively in the absence of a validated quantitative criterion and may provide additional diagnostic information in some cases. A comparative analysis with the contralateral side is often very useful.

All studies agree that in the absence of a consensus about the diagnostic ultrasound criteria and in view of the recognized performance of EMG, it cannot at present be replaced by ultrasound [56]. Whilst EMG provides important prognostic information before surgical release regarding the severity of nerve damage, ultrasound is difficult to use in this situation because of conflicting results [57—60]. One indisputable advantage of ultrasound, however, is its ability to depict a compressive mass. Of these, supernumerary muscles are a rare cause of CTS occurring on effort and resolving at rest. The muscles must be seen within the carpal tunnel in the resting position to be incriminated as the cause of CTS. Other masses arising both from joints (cysts or synovial tumors), or in the tendon sheaths (tenosynovitis, sheath tumors, etc.) may be seen on ultrasound (Fig. 5). Two tips can be recommended for this on ultrasound examination of the carpal tunnel. In order to circumvent the anisotropism of the flexor tendons due to their oblique path running deeply, the first tip is to incline the probe upwards and downwards to recognize them and ensure that there is no ectopic mass non-subject to the anisotropic effect present in the canal. The second tip is to examine the canal to its distal end in order to not miss a deep compressive lesion vel.

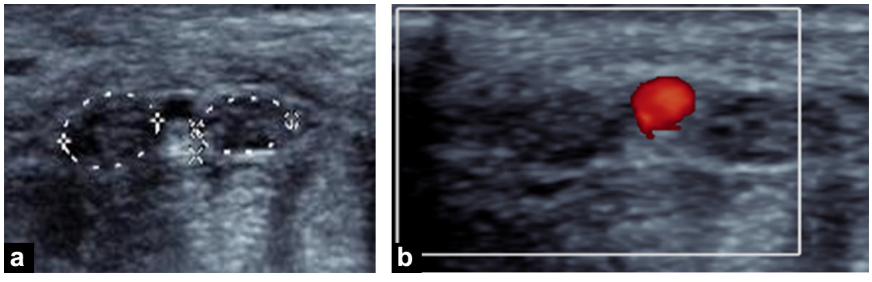

Figure 3. Bifid median nerve in a patient with carpal tunnel syndrome confirmed on electromyogram. a: on B mode ultrasound, the sum of the cross-sectional areas of the two components (dots) is measured (in this patient the surface is 12 mm^2); b: Doppler ultrasound in power mode confirms patency of median artery.

Table 1 Studies reporting diagnostic performance of ultrasound for the diagnosis of carpal tunnel syndrome (CTS).

Authors (year)	Number CTS/controls	Diagnostic reference	CSA (mm^2)	Se (%)	Sp (%)	Comments Other parameters (Se/Sp %)
Duncan et al. (1999) [33]	102/68	EMG	9	82	97	FI > 3.3 (38/75)
Ziswiler et al. (2005) [38]	78	Clinical and EMG	10	82	87	
Wong et al. (2004)	193/35	Clinical and EMG	CSp > 9 or CSd > 12	94	65	BR > 2.5 mm (0. 74/0.59) on R, (0.61/0.45) on L
			10	83	73	TR > 0.95 mm (0.64/0.36) on R, (0.65/0.38) on L
Ooi et al. (2014) [17]	95/30	Clinical and EMG	9.8	88	94	FI > 3.4 (65/60) Hypervasc. (69/95)
El Mediany et al. (2004) [36]	96/156	Clinical and EMG	10	98	100	
Visser et al. (2008) [40]	168	Clinical and EMG	10	78	91	CSAmax/AB > 2 (69/90) Measured in distal 1/3 forearm
Wang et al. (2008) [32]	61/40	Clinical and EMG	9.9	82	87.5	
Yesildag et al. (2004) [37]	148/76	Clinical and EMG	10.5	89	94	FI > 3 (37/85)
Ghasemi-Esfe et al. (2011) [18]	101/55	Clinique	10.5	71	91	Hypervasc. (83/89)
Sarria et al. (2000) [35]	64/42	Clinical and EMG	11	73	57	BR > 2.5 mm (81/64)
Wiesler et al. (2006) [39]	44/86	Clinical and EMG	11	91	84	
Mallouhi et al. (2006) [19]	172	Clinical and EMG	11	91	47	FI > 3 (60/76). BR > 2 mm (65/68) HypoE (80/65) Hypervasc. (95/71)
Klauser et al. (2009) [42]	100/93	Clinical and EMG	11	99	86	
			Delta CSA > 2	99	100	
Hunderfund et al. (2011) [43]	55/49	EMG	11	84	84	CSAmax/AB > 2.4 (67/86)
			Delta CSA $\geq$ 6	82	84	AB: middle of forearm
Tajika et al. (2013) [44]	50/81	Clinical and EMG	11	86	91	AB: distal radio-ulnar joint
			Delta CSA > 2	100	99	
Moran et al. (2009) [41]	46/50	EMG	CSA $\geq$ 12.3 mm2	62	95	Measurement includes hyperechogenic epineural ring
Nakamichi et al. (2002) [14]	414/408	Clinique	13	57	97	235 women/40 men
Lee et al. (1999) [34]	65 CTS	EMG	15	88	96	32% patients with severe EMG damage

CSA: cross-sectional area; number CTS: number of Carpal Tunnel Syndromes (wrist); EMG: electromyogram; Se: sensitivity; Sp: specificity; FI: flattening index; BR: bulging of the flexor retinaculum; TR: thickness of the retinaculum; hypervasc.: intra-neural Hypervascularization; HypoE: hypoechogenicity of the median nerve; CSAmax/AB: ratio of the maximum median nerve MN CSA at the wrist/MN CSA in the forearm; delta CSA: difference between maximum MN CSA at the wrist and MN CSA at the forearm or at the wrist.

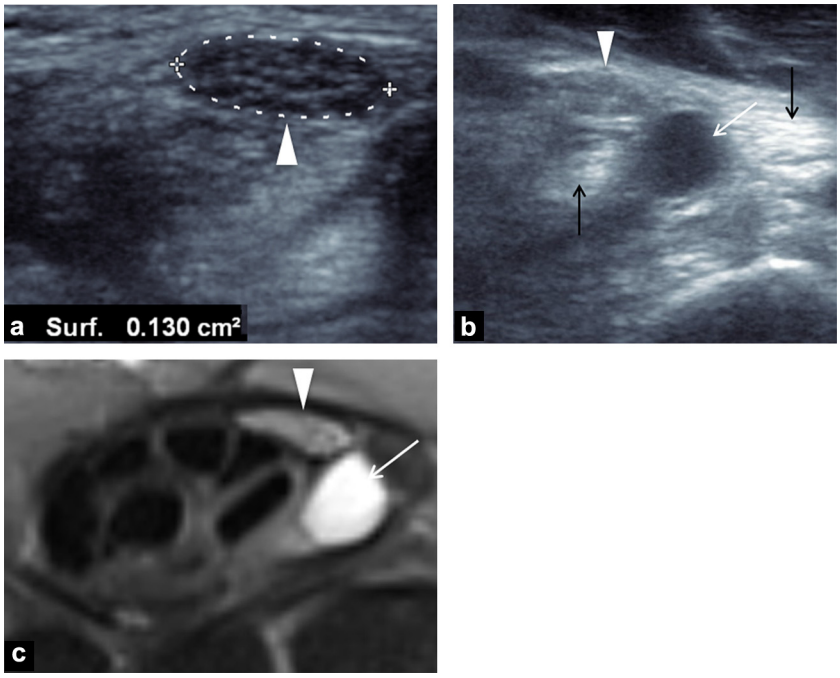

Figure 4. Left carpal tunnel, atypical considering gender and the young age in a 33-year-old man, revealing a deep palmar arthrosynovial cyst located at the distality of the carpal tunnel. a: ultrasound shows median nerve (arrowhead) with increased diameter; b: performing tilting movements with the probe allows bringing up tendons (black arrows), subject to anisotropy, hyperechoic. Thereby, it is easier to distinguish the anechoic cyst (white arrow) from them; c: fat-saturated proton density-weighted image in the transverse plane shows the compressive arthrosynovial cyst (white arrow). Increased signal intensity of the median nerve may indicate distress (arrowhead).

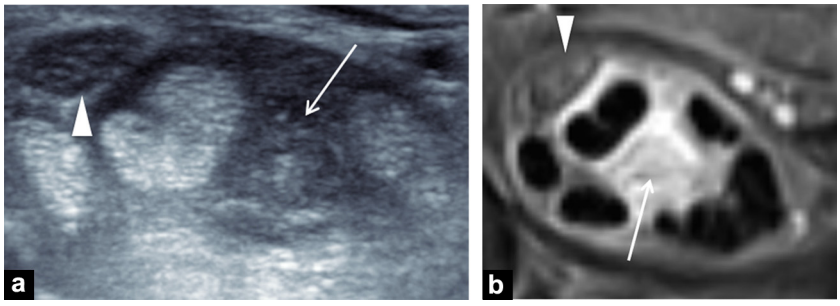

Figure 5. Carpal tunnel syndrome on exertion revealing tenosynovitis of the flexors combined with a compressive mass in the carpal tunnel suggestive of GCT. Pathological anatomy concluded an inflammatory fleshy bud due to non-specific synovitis. a: ultrasound shows hypoechogenic thickening of the common superficial flexor tendon sheaths and central hypoechogenic mass (white arrow); b: fat-saturated proton density-weighted image in the transverse plane shows a synovial mass (white arrow). The median nerve (arrowhead) shows normal signal intensity.

MRI

MRI offers a poorer spatial resolution than ultrasound. It is of limited use to make a positive diagnosis of CTS [6,22] and is performed as a second-line examination, particularly to identify a cause of extrinsic compression seen on ultrasound [59].

Postoperative imaging

Postoperatively, the time course of symptoms is helpful to determine the actual cause. Identical persistence of symptoms suggests incomplete section of the flexor retinaculum, nerve compression at a site other than the carpal tunnel suggests iatrogenic nerve damage (rare) or a compressive mass which has been missed before surgery. Recurrent symptoms after a symptom-free period should suggest perineuronal fibrosis.

Whilst ultrasound has an indisputable role in the diagnosis of a compressive mass, its performance in diagnosing persistent nerve distress and inadequate surgical release is less certain. Whilst several authors have shown that a median nerve operated on successfully tends to reduce gradually in thickness over the weeks after surgical release [61—64], others have shown an increase in CSA despite recovery [65]. The utility of such ultrasound monitoring is hindered by the fact that preoperative ultrasounds are often not present in the patients' records. In any event, isolated use of the postoperative CSA is difficult as a nerve which has been distressed for a period of time appears to retain some scar-

ring hypertrophy despite symptoms disappearing [64—66]. In a prospective series of 24 patients and 44 wrists treated surgically, Kim et al. reported a mean preoperative CSA of 14.5 mm^2, compared to 13 mm^2 at 3 weeks and 11.5 mm^2 at 3 months after surgery [67]. The presence of increased signal intensity of the nerve on T2-weighed images is not specific after surgery [30].

Inadequate median nerve release is difficult to assess by imaging. This is suggested on MRI when the median nerve and most palmar flexor tendons are located on the surface of a line joining the trapezium and hamate in the transverse plane [30]. In our experience inadequate transverse translation of the nerve during flexion-extension finger movements on ultrasound is a useful sign, but highly subjective (Fig. 6).

Perineuronal fibrosis is relatively straightforward to diagnose on imaging. It appears on ultrasound as an irregular, poorly delineated hypoechogenic perineuronal area fixing the nerve during dynamic finger flexion-extension movements. It may adjacent to the palmaris longus on the surface (superficial fibrosis) or in contact with the flexor tendons (deep fibrosis). On MRI, perineuronal fibrosis presents as a poorly delineated, low intensity area on T1- and T2-weighted image, that shows enhancement after intravenous administration of a gadolinium chelate [30].

Median nerve at the elbow

Compression of the median nerve at the elbow is very rare. Three main compression sites are found. They include the path beneath the aponeurotic expansion of the biceps or lacertus fibrosus, promoted by a thickening scar; the path between the humeral and ulnar heads of the pronator teres, which is the most common; and the fibrous arch of the superficial finger flexor, more distally. The second two of these are grouped into the same clinical entity called the pronator teres syndrome. This may be secondary to repeated pronation-supination movements when the humeral (or superficial) head of the pronator teres applies repeated mechanical compression onto the median nerve.

The supracondyloide process syndrome is secondary to a rare anatomical variant and involves compression of the median nerve in a tunnel formed by the bony spur of the same name arising 5 cm above the medial epicondyle, which is clearly visible on plain radiographs and is prolonged by a Struthers ligament which returns to the medial epicondyle.

Ulnar nerve at the elbow

The ulnar tunnel syndrome (UTS) is the second most common upper limb neuropathy. The ulnar tunnel is delineated internally by the posterior bundle of the ulnar collateral ligament and the joint capsule and externally by the ulnar tunnel retinaculum (formerly the ligament of Osborne) which runs between the olecranon and the medial epicondyle. This retinaculum may be absent, which predisposes to anterior luxation of the nerve, or it may be replaced by the medial aconeous muscle which is present in 3 to 28% of people [68]. The diagnosis of ulnar tunnel syndrome is based on a combination of a detailed clinical examination, EMG and ultrasound.

Pathophysiology

Damage to the ulnar nerve at the elbow occurs as a result of different isolated or combined mechanisms including compression, stretching and friction. The volume of the tunnel reduces in flexion as a result of the ulnar tunnel retinaculum being placed under tension and bulging of the medial collateral ligament causing increased pressure in the tunnel with a risk of compression following prolonged or repeated elbow flexion. Any compressive structure in the tunnel may also be involved, both constitutional (medial aconeous muscle, defective hollowing of the medial epicondyle or congenital hypoplasia of the trochlea) or acquired (thickening of the medial collateral ligament, epicondylar groove osteophyte, synovial pannus, cysts etc.). Friction is secondary to nerve instability in flexion which is then located across the apex of the medical epicondyle (subluxation) or anteriorly (luxation). The frequency of subluxation on ultrasound is 14—27% compared to 6.7—20% for luxation in both asymptomatic people and patients [3,69—71]. Its role in development of symptoms, however, is debated in view of the high prevalence of instability in asymptomatic people (16% subluxation) [3].

Imaging

Ultrasound

In the normal state, the average CSA of the ulnar nerve next to the medial epicondyle immediately proximal to the ulnar tunnel ranges between $6.6 \pm 1.7\ mm^2$ and $7.9 \pm 3.1\ mm^2$ [4,69]. Several large bundles can occasionally be seen and are of no pathological significance [4,69]. Beyond 90° flexion, the nerve flattens physiologically [69,72]. An increase in the CSA is the best indicator of ulnar nerve distress although

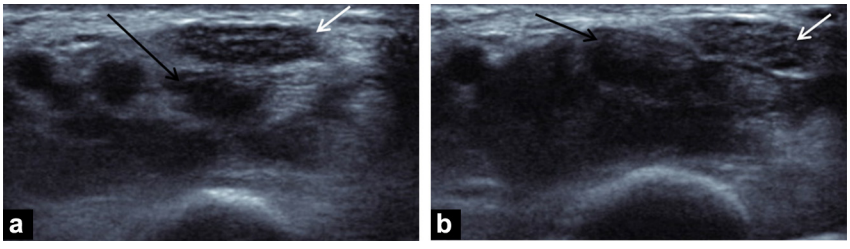

Figure 6. Dynamic ultrasound during flexion-extension movement of the fingers shows good mobility of the median nerve (white arrow) in the transverse plane on a background of persistent symptoms after carpal tunnel surgery. This argues, in our experience, against a nerve release failure. a: normal position of the median nerve during fingers extension; b: normal lateral translation of the median nerve above superficial flexor tendons (black arrows) during fingers flexion.

there is no consensus about the best cut-off value [72—81]. However, a value of 10 or even 11 mm^2 appears to offer a good compromise (Fig. 7) (Table 2).

Similar to the carpal tunnel, a comparison of maximum CSA of the nerve at the elbow against a reference value for a given patient measured in the forearm or middle third of the humerus is proposed by some authors and offers good diagnostic performance with a thickening ratio > 1.5 [74,77,79]. However, it does not appear to perform better than measuring the CSA alone only at the site of maximum thickening, although may be particularly useful in unusually short or tall people. Ultimately, the simultaneous use of the CSA value and a CSA ratio would offer the best diagnostic performances [74,76,79].

A dynamic study should be performed routinely during ultrasound in order to search for instability of the nerve, which although of uncertain pathological significance needs to be known by the surgeon (Fig. 8).

MRI

MRI must be performed with the elbow in extension. The ulnar nerve is identified on T1-weighted images as a round or ovoid structure. The isolated presence of an increased intensity of the nerve on T2-weighted images at the level of the medial epicondyle should not lead to the diagnosis of UTS as this is seen in 60% of asymptomatic people [7]. A raised signal intensity of muscle on STIR images reflects denervation of the flexor carpi ulnaris, the deep finger flexor and the intrinsic muscles of the hand which depend on the ulnar nerve [6,29].

Postoperative imaging

There is limited available data in the literature on the ultrasound appearances of an ulnar nerve after neurolysis or anterior transposition whether or not the outcome is satisfactory. In our experience, morphological abnormalities of the nerve may last for a long period of time after surgery. Recurrence of UTS due to formation of a new sheath site may occur in which case imaging may help to establish the specific site of the nerve distress before surgery [26].

Ulnar nerve at the wrist: Guyon's tunnel syndrome

This is the second ulnar nerve compression site in the upper limb. It is rarely idiopathic and any mass in the proximal Guyon's tunnel can compress the nerve (cyst, venous malformation or supernumerary muscle). Anatomical variants at this point are very common particularly an accessory 5th finger accessory abductor muscle (24% in a series of asymptomatic patients) (Fig. 9) [82]. This is only rarely responsible for nerve compression. In the distal canal or more distally in the palm of the hand the superficial branch of the nerve is vulnerable to direct injuries.

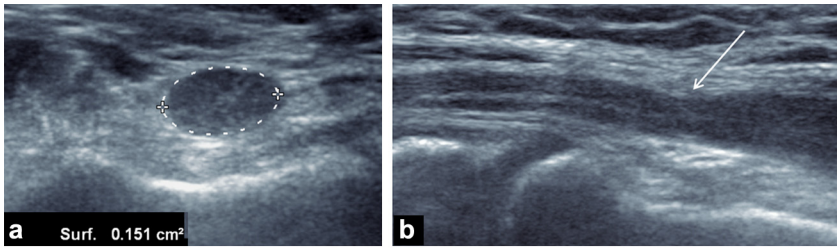

Figure 7. Signs of nerve distress on ultrasound in a patient with ulnar tunnel syndrome confirmed on electromyogram. a: ultrasound image in the transverse plane shows a cross-sectional surface area of 15 mm^2 and hypoechogenicity of the nerve. b: longitudinal section: increased diameter of the nerve immediately proximal to its path beneath the presumed position of the ulnar tunnel retinaculum (arrow).

Table 2 Studies on the diagnostic performance of ultrasound for the ulnar tunnel syndrome (UTS).

Authors (year)	Number of UTS/controls	Diagnostic reference	CSA (mm^2)	Se (%)	Sp (%)	Comments Other parameters (Se/Sp %)
Mondelli et al. (2008) [73]	33/14	EMG	8.8	46	NR	
Yoon et al. (2008) [74]	26/30	EMG	8.3	100	93	CSAmax/(A or FA) > 1.5 (100/97)
Volpe et al. (2009) [75]	50/50	EMG	10	88	88	
Bayrak et al. (2010) [76]	41/42	EMG	11	95	71	P/CSAmax < 0.4 (86/59)
Gruber et al. (2010) [77]	41/45	EMG	NR	NR	NR	CSAmax/A > 1.4 (54/96)
Ayromlou et al. (2012) [73]	29/35	EMG	6	93	68	CSAmax controls < published data (5 mm^2)
Pompe et al. (2013) [79]	137/73	Clinical and/or EMG	10	56	81	CSAmax/A > 2.3 (57/77)
Kim et al. (2015) [80]	25/30	EMG	9	93.8	88.3	CSAmax/FA > 1.5 (93.8/95)

CSA: cross-sectional surface area; EMG: Electromyogram; Se: sensitivity; Sp: specificity; NR: not recorded; CSAmax/A: ratio of maximum ulnar nerve (UN) CSA at the elbow to NU CSA at mid-humerus; CSAmax/FA: ratio of maxCSA to max UN CSA in the forearm; P/CSAmax: ratio of UN CSA at the wrist to CSAmax.

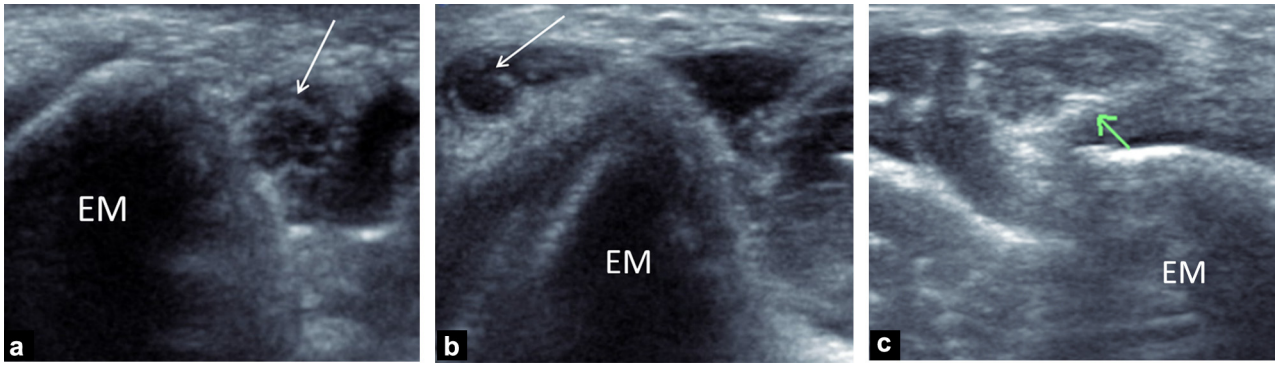

Figure 8. Cases of unstable ulnar nerves (UN) revealed by dynamic ultrasound maneuver. a: case 1, axial view in flexion under 90°: UN (white arrow) in the anatomical position; b: case 1, forced elbow flexion: luxation of the UN in front of to the medial epicondyle. c: case 2: subluxation of the UN (green arrow) during forced elbow flexion, lying above the medial epicondyle (ME), in this case on the left.

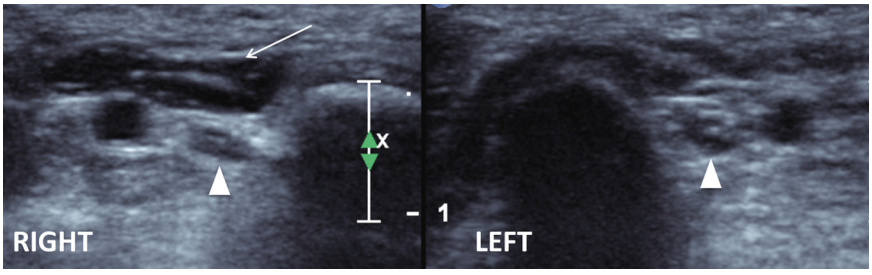

Figure 9. Comparative ultrasound appearance of right and left Guyon's tunnels showing an asymptomatic accessory 5th finger abductor muscle (white arrow) on the right, with no compression of the ulnar nerve (arrowhead), discovered fortuitously.

Ultrasound is the first-line imaging modality to investigate the nerve although MRI can be effective in examining the hypothenar region [83]. Whilst the usual signs of nerve distress may be seen, ultrasound is used mostly to identify an extrinsic compressive mass (Fig. 10). MRI should be used in atypical situations, when the EMG is non-contributory, or if a tumour is found on ultrasound.

Radial nerve at the elbow

Anatomical and clinical aspects

At the elbow, the radial nerve divides into a superficial sensory branch and a deep motor branch known as the posterior interosseous nerve. Damage to the radial nerve at this point may result in two different clinical pictures: the radial tunnel syndrome which involves mostly pain and mimics lateral epicondylitis and the posterior interosseous nerve syndrome which is rarer and paralytic (usually of traumatic origin).

The most classical compression site is Fröhse's arcade which is the proximal edge of the superficial head of the supinator muscle although passing next to the radio-capital joint the fibrous edge of the extensor carpi radialis brevis tendon, the presence of a recurrent radial artery (or ''leash of Henry'') and the distal edge of the supinator muscle have occasionally been implicated. Repeated pronation-supination movements can promote development of a tunnel syndrome. Compression by a mass is rarer.

Imaging

Whilst ultrasound performs well for the detection of median and ulnar nerve tunnel distress due to a tunnel syndrome, the same does not apply to the radial nerve, particularly

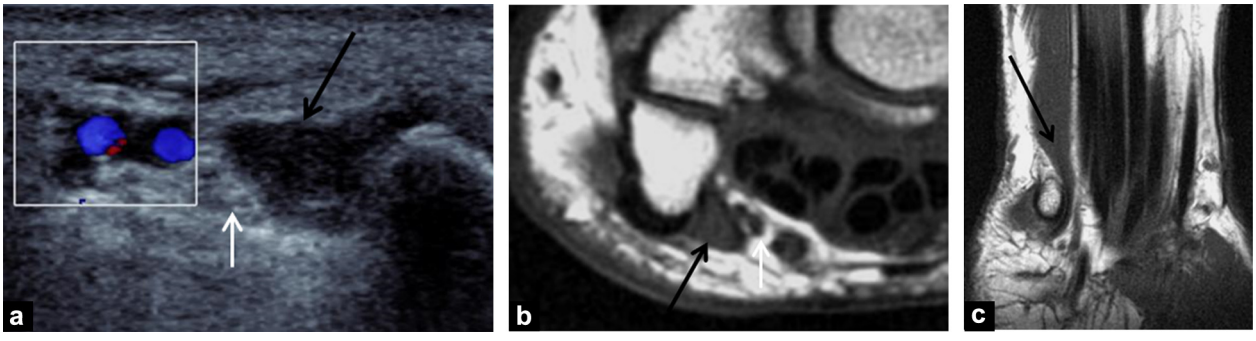

Figure 10. Guyon's tunnel syndrome due to a compressive accessory 5th finger long flexor muscle. a: ultrasound shows muscle mass (black arrow) in Guyon's tunnel adjacent to the ulnar nerve (white arrow); b: T1-weighted images in the (b) axial and (c) coronal planes show the accessory muscle (black arrow) in the Guyon tunnel, adjacent to the ulnar nerve (white arrow).

because of the high prevalence of physiological bulge of the nerve proximal to Fröhse's arcade in our experience, casting considerable doubt on the positive predictive value of this sign (Fig. 11). At present, there are no controlled studies on this sign or reliable cut-off value.

On MRI, denervation muscle edema of the supinator muscle and of the forearm extensor muscles is the most common finding, observed in 52% of patients (Fig. 12) [84]. MRI of the elbow with use of T1-weighted and STIR images centered on the muscles appear to us as the examination of choice when a radial nerve tunnel syndrome is clinically suspected. Ultrasound and MRI are also used to exclude a compressive mass (Fig. 13).

Radial nerve at the forearm

Wartenberg's syndrome involves damage to the superficial sensory branch of the radial nerve in the distal third of the forearm. This is a differential diagnosis of De Quervain's tendinitis and the crossover of the radial nerves with the extensor pollicis brevis and abductor pollicis longus. Whilst entrapment neuropathy is very rare at this level, traumatic injury is far more common in view of its superficial path towards the wrist.

Future prospects

The role of diffusion tensor imaging has been evaluated in several studies on the peripheral nerves, particularly the median nerve in the carpal tunnel. Researchers have shown a significant reduction in the anisotropic fraction in CTS [85]. Further studies are needed to establish nominal values and pathological cut-offs for each peripheral nerve and compression site.

Elastosonography can show a drop in the elasticity of the pathological median nerve [86]. Nerve supporting tissue fibrosis as a response to interstitial edema and nerve traction lesions is a further parameter that can be used to assess nerve distress.

Traumatic and iatrogenic nerve injuries

Traumatic damage to a peripheral nerve is not particularly rare and has been estimated to occur with an incidence of 13.9/100,000/year in a Swedish study whereas its

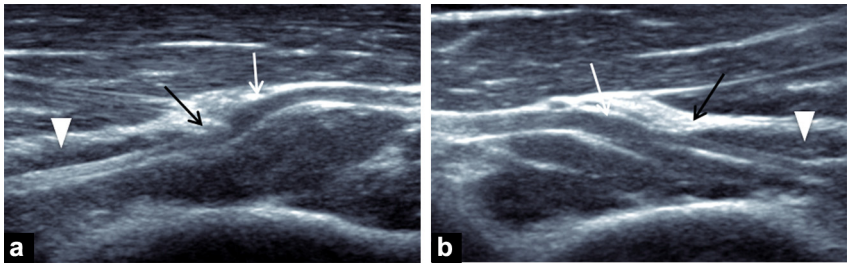

Figure 11. Local thickening of the deep branch of the radial nerve at the elbow, doubtful, in a context of lateral epicondylar pain resistant to medical treatment, not shown to be a radial tunnel syndrome on electromyogram. a: longitudinal ultrasound on the symptomatic right side: local thickening of the nerve (white arrows) as it passes beneath the Fröhse arcade (black arrows). Superficial head of the supinator muscle (arrowhead); b: the comparison with contralateral asymptomatic side shows a similar appearance.

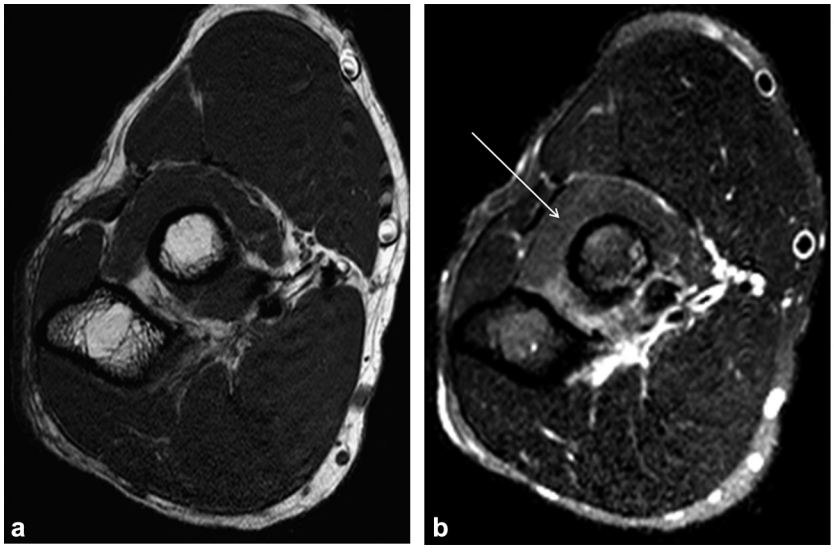

Figure 12. MR imaging shows signs of denervation of the supinator muscle in a patient with atypical lateral epicondylar pain suggestive of radial tunnel syndrome. a: T1-weighted MR image in the transverse plane shows no abnormal muscle degeneration; b: T2-weighted STIR image in the transverse plane shows increased signal intensity in the supinator muscle (arrow).

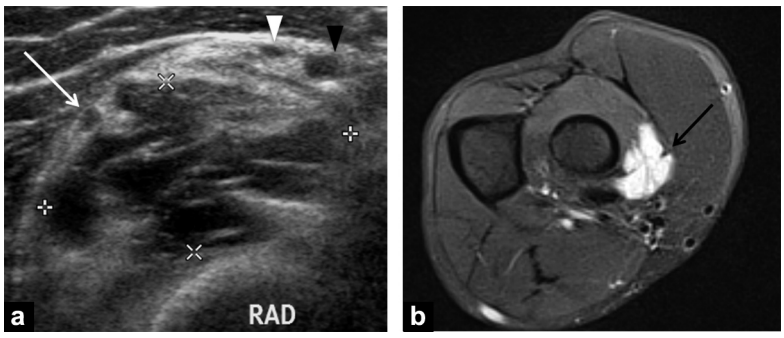

Figure 13. Exploration of a right radial tunnel syndrome revealing an athrosynovial cyst, confirmed by histology. a: ultrasound in the transverse plane shows hypoechogenic, multilobulated mass involving the deep fibers of the supinator muscle (delineated by the crosses) pushing the deep branch (DB) of the radial nerve (white arrow) forwards. Superficial branch of the radial nerve (white arrowhead) and recurrent radial artery (black arrowhead). b: fat-saturated proton density-weighted image in the transverse plane shows a multilobulated very high signal intensity mass corresponding to the cyst (black arrow).

prevalence may be as high as 2% [87]. Despite care in identifying and protecting neuronal tissues during surgery, iatrogenic injuries are common and account for 17.4% of surgical nerve damage [88]. There are many isolated or combined mechanisms for the injury including partial or total division, stretching, compression, thermal or chemical burns and occasionally ischemia of the nerve [87].

Acute nerve injuries

Trauma may be direct — either open (a penetrating wound or open fracture), or closed — or indirect due to stretching (luxation). Among bone fractures, humeral fracture causes injury to the radial nerve, which passes immediately next to it, with an incidence ranging between 2 and 18% (Fig. 14)

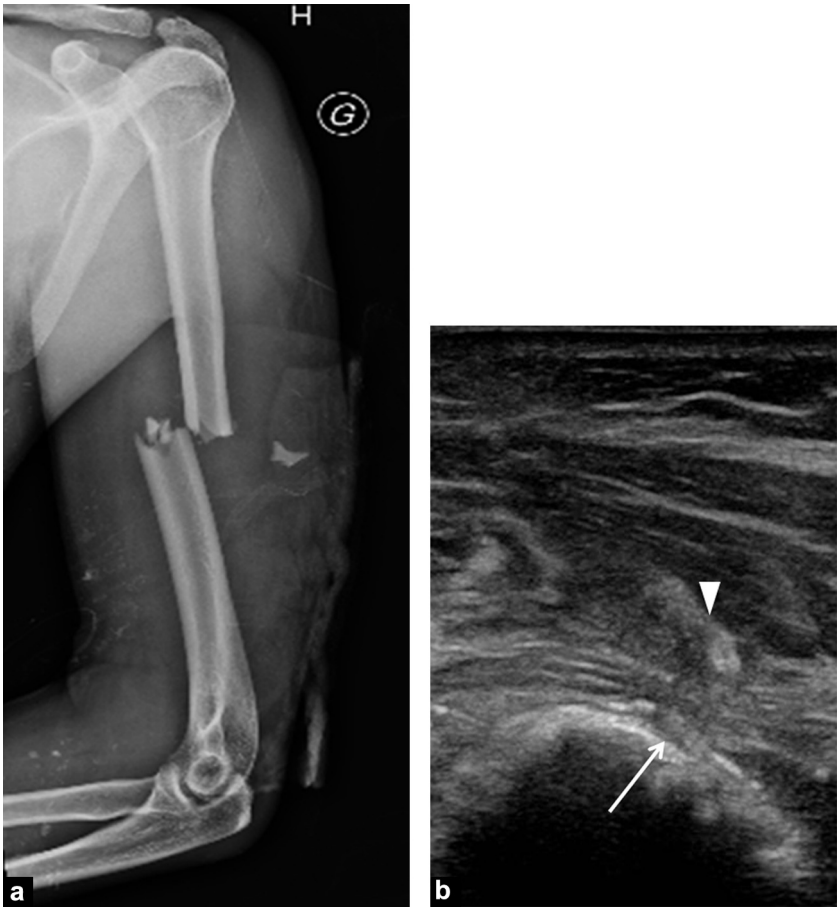

Figure 14. Paralysis of the left hand and wrist extensors 10 days after an open fracture treated by anterograde pinning in a patient with multiple trauma. a: radiograph of the displaced diaphyseal left humeral fracture; b: ultrasound image in the axial plane shows radial nerve damage (white arrow), grade 4 of the Sunderland classification: focal narrowing of the nerve with interruption of the epineuron and loss of fasciculated appearances reflecting damage to the perineuron combined with interruption of the brachial triceps (arrowhead) which suggests it passes through the bone, with damage to the muscle.

[89]. It is fundamental in the initial management of an acute nerve injury to establish the degree and type of nerve damage because they have impact on treatment options. In this regard, the greater the disorganization of the neuronal tissue, the less will be the response of the nerve following wallerian degeneration decrease with increasing disorganization of the neuronal structure. Acute nerve injuries were initially categorized into three types of injuries (neurapraxia, axonotmesis and neurotemesis), and further into five levels (Table 3) [90]. Treatment involves operating on severe irreversible lesions within 24—72 h, to reduce fibrosis and nerve retraction [87,90].

Imaging can be used to assess the severity of nerve injury, measure its extent and identify muscle degeneration from 48 h onwards and exclude a compressive effect (hematoma or collection) explaining the deficit [87]. However, there are inconsistent reports about the utility of acute phase ultrasound for an open injury. For some authors, ultrasound is the perfect approach offering a detailed analysis of the whole nerve and of its relationships with neighboring structure [91], whereas others reported a sensitivity of 75% only and a specificity of 91% [92]. Limiting factors are predominantly obesity, posttraumatic edema and a need for a well-trained operator [85]. MRI is mostly limited by its poor spatial resolution, particularly in investigating digital nerve lesions [91—93]. Ultrasound and MRI appearances are given in details in Table 3 [87].

Chronic nerve lesions

''Neurogenic'' pain next to or around a surgical scar occurs with an incidence ranging from 10 to 50% [94]. Subcutaneous sensory nerves account for almost 33% of iatrogenic nerve injuries [88]. The main upper limb subcutaneous nerves and types of procedures involved are reviewed in Table 4.

Causative nerve lesions include neuromas, in continuity (secondary to incomplete division) or terminal discontinuity (secondary to complete division) and scarring fibrous sheathing tightening the nerve endings. Neuroma is a bulbar structure originating from normal healing of a nerve after its division in response to various neurochemical factors [94]. In 3—5% of cases it causes intense neuropathic pain which may be pharmacologically difficult to relieve and a source of incapacity and significant medical and social costs [95,96].

Imaging, particularly ultrasound, provides essential information for treatment planning by detailing the exact site of the lesion, the extension and type of neuronal lesion (neuroma or fibrosis) and also its responsibility for pain at the

Table 3 Classification of traumatic nerve injuries [85].

Type of injury (Seddon)	Degree of injury (Sunderland)	Pathophysiology	Electromyography	Nerve imaging (MRI/ultrasound)	Muscle imaging (MRI/ultrasound)	Recovery time
Neurapraxia	I	Segmental demyelination without axonal rupture	Local block or slowing of conduction	Normal	Normal	Up to 3 months
Axonotmesis	II	Axonal rupture	No neuronal conduction distal to the lesion, muscle denervation	Enlarged hyperintense on T2 imaging or hypoechogenic Loss of fascicular structure May be normal or partial continuity due to neuroma	Denervation edema (hyperintense on T2) Return to normal possible or progression to chronic denervation	Variable depending on degree of injury and site (nerve response 1 mm/day)
	III	Axonal and endoneuronal rupture				
	IV	Axonal, endoneuronal and perineuronal rupture				
Neurotmesis	V	Complete rupture of nerves	Idem	Nerve continuity solution Terminal neuroma	Chronic denervation (atrophy and fatty replacement hyperintense on T1)	No spontaneous recovery

Table 4 Types of surgery resulting in iatrogenic injuries to the upper limb subcutaneous nerves.

	Nerves	Type of surgery	Most common sensory territory
Elbow			
	Lateral cutaneous nerve of the forearm	Surgical repair of ruptured brachial biceps tendon	Anterior and posterior radial aspects of the forearm
		Elbow arthroscopy (lateral approach)	From the antecubital fossa to the thenar eminence
	Superficial branch of the median nerve	Surgical repair of a rupture brachial biceps tendon	Radial aspect of the hand and dorsal aspect of the thumb
		Elbow arthroscopy (lateral approach)	From the index finger and lateral side of the middle finger to the distal interphalangeal joint
Wrist—hand			
	Lateral cutaneous nerve of the forearm	Surgical treatment of fractures of the distal end of the radius	Anterior and posteriors aspects of the forearm from the antecubital fossa to the thenar eminence
		Carpometacarpal approach to the 1st digit, open or arthroscopic	
		Decompression of 1st extensor cavity	
		Blood gases, radial artery catheterisation	
	Palmar cutaneous branch of the median nerve	Surgery to the radial aspect of the wrist	Palmar surface lateral to the midline of the 4th finger
	Superficial branch of the radial nerve	Surgery to the radial aspect of the wrist	Radial aspect of the hand and distal surface of the thumb
		Lateral approach to the radius	From the index and lateral half of the middle finger to the distal interphalangeal joint
		Surgery to the carpometacarpal joints and metacarpophalangeal joints of the thumb	
		Canulation, injection of the cephalic vein, dialysis fistula	
		Blood gases, radial artery catheterisation	
	Dorsal cutaneous branch of the ulnar nerve	Surgery to the distal end of the ulna	Dorsal ulnar aspect of the hand
		Articular approach to the wrist, open or arthroscopic	Dorsal aspect of the 5th finger
		5th finger surgery	Dorsal ulnar aspect of the 4th finger
		Extensor tendon surgery	

Figure 15. Fusiform neuroma in the dorsal cutaneous branch of the ulnar nerve following direct pinning of a fracture of the base of the fifth metacarpal bone and the hamatum. a: postoperative radiograph; b: fusiform neuroma of the dorsal cutaneous branch of the ulnar nerve; c: photograph of operation scar, which helps to localize the neuroma.

trigger point (Fig. 15). The treatment of scarring pain due to fibrous perineuronal sheathing mostly involves exoneurolysis.

In conclusion, imaging has now an undisputable role in the assessment of the main causes of upper limb nerve distress. MRI is a useful adjunct for the investigation of nerves and the assessment of the consequences on muscles. However, ultrasound remains the first-line imaging technique because it can provide morphologic and dynamic information. In addition, its unsurpassed spatial resolution allows examination of deep and subcutaneous nerves. New techniques such as elastography and MRI tractography are being investigated but require further studies.

Take-home messages

Carpal tunnel syndrome

- Ultrasound is part of a diagnostic approach combining clinical examination and electromyography (EMG). Ultrasound is only indicated in atypical clinical presentation with symptoms due to effort or recurrence/persistence after surgery.
- Ultrasound is used particularly to search for signs of nerve distress and determine the cause of nerve compression.
- Nerve hypertrophy is the most specific ultrasound finding of nerve distress is. The use of a delta cross-sectional surface area shows promise because of its excellent diagnostic performance.
- Anisotropism needs to be taken into account when investigating for a mass in the carpal tunnel by ultrasound to detect this within the flexor tendons, whereas scanning mode should be used for the tunnel to its distal end in the palm of the hand.

Ulnar tunnel syndrome

- Ultrasound is performed routinely after surgery in order to confirm nerve distress, investigate for a compressive mass and estimate nerve stability.
- Although EMG is reliable in localizing, examination of the nerve throughout its length as far as the Guyon's tunnel should be performed routinely in order to not miss an extrinsic mass or neurogenic nerve tumor.
- Nerve stability in flexion should be assessed by a dynamic investigation as, according to some surgeons, this influences the operation technique.

Radial tunnel syndrome

- Radial nerve distress at the elbow due to compression of its deep branch beneath the Fröhse arcade is a rare cause of lateral epicondylar pain.
- Ultrasound has limited value because of the limited positive predictive value of nerve hypertrophy, which is very often present in asymptomatic people. EMG is poorly sensitive.
- MRI of the elbow is a valuable tool to guide the diagnosis when signs of supinator muscle denervation are present.

Traumatic nerve injuries
- Because of its good spatial resolution, ultrasound can be used to provide a detailed assessment of acute and chronic nerve injuries.
- In the acute phase it assesses the type (division, stretching or compression) and extent of the injury.
- In the chronic phase it is used to look for a neuroma and determine whether the nerve is partially or totally discontinuous and assesses the extent of any concomitant peripheral fibrosis.

Clinical case

A 71 year-old-woman underwent surgery 6 months ago for clinically typical left carpal tunnel syndrome that was confirmed by EMG. Despite surgery, she consulted 4 months later for persisting similar symptoms. Ultrasound examination was requested (Fig. 16).

Questions

1. Would the patient have benefitted from preoperative imaging?

2. Does postoperative ultrasound allow drawing a conclusion regarding persistent nerve distress?

3. In view of ultrasound findings, the patient underwent MRI examination (Fig. 16). Which of the following proposed diagnoses would you make?
- palmar arthrosynovial cyst of the wrist;
- supernumerary muscle;
- synovitis of the wrist;
- algodystrophy;
- scarring perineural fibrosis.

Answers

1. No. According to the March 2013 HAS guidelines imaging is useless in carpal tunnel syndrome when the clinical presentation is typical [30].

2. No, persistent ultrasound signs of nerve distress appearing as a borderline cross-sectional surface area and hypoechogenicity of the nerve do not allow concluding that the damage is persistent, as moderate thickening of the nerve may be seen during the initial months after surgery [64—67]. It is difficult to interpret this sign because the patient did not have a reference ultrasound before surgery.

3. Ultrasound and MRI show palmar synovial thickening of the wrist with peripheral enhancement on MRI after intra-

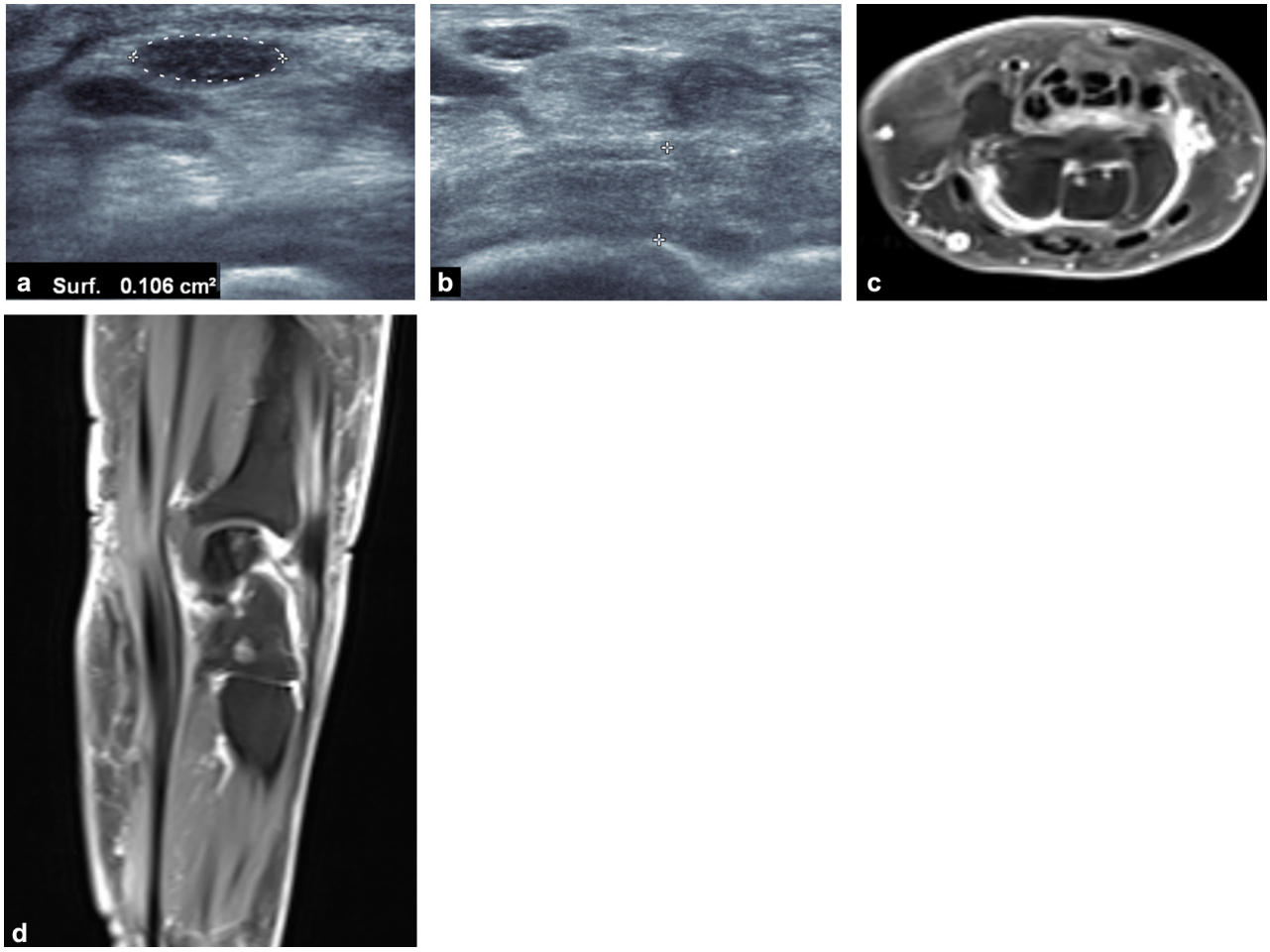

Figure 16. Clinical case: postoperative ultrasound and MRI. a, b: ultrasound images in the transverse plane; c, d: fat-saturated T1-weighted images in the (c) sagittal and (d) transverse planes obtained after intravenous administration of a gadolinium chelate.

venous administration of a gadolinium chelate suggestive of synovitis of the wrist. This clinically unapparent synovitis probably contributed to the development and persistence of the patient symptoms because of the mass effect on the carpal tunnel.

Disclosure of interest

The authors declare that they have no competing interest.

References

[1] Kirchgesner T, Pesquer L, Larbi A, et al. Axial traction in magnetic resonance arthrography of the wrist: how to do? Diagn Interv Imaging 2015;96:519—22.
[2] Lundborg G, Dahlin LB. Anatomy, function, and pathophysiology of peripheral nerves and nerve compression. Hand Clin 1996;12:185—93.
[3] Okamoto M, Abe M, Shirai H, Ueda N. Morphology and dynamics of the ulnar nerve in the cubital tunnel. Observation by ultrasonography. J Hand Surg [Br] 2000;25:85—9.
[4] Jacob D, Creteur V, Courthaliac C, Bargoin R, Sassus B, Bacq C, et al. Sonoanatomy of the ulnar nerve in the cubital tunnel: a multicentre study by the GEL. Eur Radiol 2004;14:1770—3.
[5] Thoirs K, Williams MA, Phillips M. Ultrasonographic measurements of the ulnar nerve at the elbow: role of confounders. J Ultrasound Med 2008;27:737—43.
[6] Andreisek G, Crook DW, Burg D, et al. Peripheral neuropathies of the median. Radial and ulnar nerves: MR imaging features. Radiographics 2006;26:1267—87.
[7] Husarik DB, Saupe N, Pfirrmann CW, Jost B, Hodler J, Zanetti M. Elbow nerves: MR findings in 60 asymptomatic subjects. Normal anatomy, variants and pitfalls. Radiology 2009;252:148—56.
[8] Chappell KE, Robson MD, Stonebrifge-Foster A, et al. Magic angle effects in MR neurography. Am J Neuroradiol 2004;25:431—40.
[9] Rydevik B, Lundborg G, Bagge U. Effects of graded compression on intraneural blood flow. An in vitro study on rabbit tibial nerve. J Hand Surg [Am] 1981;6:3—12.
[10] Sunderland S. The nerve lesion in the carpal tunnel syndrome. J Neurol Neurosurg Psychiatry 1976;39:615—26.
[11] Lundborg G, Myers R, Powell H. Nerve compression injury and increase in endoneurial fluid pressure: a miniature compartment syndrome. J Neurol Neurosurg Psychiatry 1983;46:1119—24.
[12] Kobayashi S, Meir A, Baba H, Uchida K, Hayakawa K. Imaging of intraneural edema by using gadolinium-enhanced MR imaging: experimental compression injury. Am J Neuroradiol 2005;26:973—80.
[13] Upton AR, McComas AJ. The double crush in nerve entrapment syndromes. Lancet 1973;18:359—62.
[14] Nakamichi K, Tachibana S. Ultrasonographic measurement of median nerve cross-sectional area in idiopathic carpal tunnel syndrome: diagnostic accuracy. Muscle Nerve 2002;26:798—803.
[15] Wong SM, Griffith JF, Hui AC, Lo SK, Fu M, Wong KS. Carpal tunnel syndrome: diagnostic usefulness of sonography. Radiology 2004;232:93—9.
[16] Aleman L, Berna JD, Reus M, et al. Reproducibility of sonographic measurements of the median nerve. J Ultrasound Med 2008;27:193—7.
[17] Ooi CC, Wong SK, Tan AB, et al. Diagnostic criteria of carpal tunnel syndrome using high-resolution ultrasonography: correlation with nerve conduction studies. Skeletal Radiol 2014;43:1387—94.
[18] Ghasemi-Esfe AR, Khalilzadeh O, Mazloumi M, et al. Combination of high-resolution and color Doppler ultrasound in diagnosis of carpal tunnel syndrome. Acta Radiol 2011;52:191—7.
[19] Mallouhi A, Pülzl P, Trieb T, et al. Predictors of carpal tunnel syndrome: accuracy of gray-scale and color Doppler sonography. AJR Am J Roentgenol 2006;186:1240—5.
[20] Vanderschueren G, Meys V, Beekman R. Doppler sonography for the diagnosis of carpal tunnel syndrome: a critical review. Muscle Nerve 2014;50:159—63.
[21] Monagle K, Dai G, Chu A, Burnham RS, Snyder RE, Quantitative MR imaging of carpal tunnel syndrome. AJR Am J Roentgenol 1999;172:1581—662.
[22] Fleckenstein JL, Wolfe GI. MRI vs EMG: which has the upper hand in carpal tunnel syndrome? Neurology 2002;58:1583—4.
[23] Jarvik JG, Yuen E, Haynor DR, et al. MR nerve imaging in a prospective cohort of patients with suspected carpal tunnel syndrome. Neurology 2002;58:1597—602.
[24] Zaidman CM, Seelig MJ, Baker JC, Mackinnon SE, Pestronk A. Detection of peripheral nerve pathology: comparison of ultrasound and MRI. Neurology 2013;80:1634—40.
[25] Kim S, Choi JY, Huh YM, et al. Role of magnetic resonance imaging in entrapment and compressive syndrome: what, where, and how to see the peripheral nerves on the muskuloskeletal magnetic resonance image. II. Upper extremity. Eur Radiol 2007;17:509—22.
[26] Subhawong TK, Wang KC, Thawalt SK, et al. High resolution imaging of tunnels by magnetic resonance neurography. Skeletal Radiol 2012;41:15—31.
[27] Bendszus M, Koltzenburg M, Wessig C, Solymosi L. Sequential MR imaging of denervated muscle: experimental study. Am J Neuroradiol 2002;23:1427—31.
[28] Polak JF, Joresz FA, Adama DF. MRI of skeletal muscle: prolongation of TI and T2 subsequent to denervation. Invest Radiol 1988;23:365—9.
[29] Kim SJ, Hong SH, Jun WS, et al. MR imaging mapping of skeletal muscle denervation in entrapment and compressive neuropathies. Radiographics 2011;31:319—32.
[30] Campagna R, Pessis E, Feydy A, et al. MRI assessment of recurrent carpal tunnel syndrome after open surgical release of the median nerve. AJR Am J Roentgenol 2009;193:644—50.
[31] http://www.has-sante.fr/portail/jcms/c_1365548/fr/syndrome-du-canal-carpien-optimiser-la-pertinence-du-parcours-patient.
[32] Wang LY, Leong CP, Huang YC, et al. Best diagnostic criterion in high-resolution ultrasonography for carpal tunnel syndrome. Chang Gung Med J 2008;31:469—76.
[33] Duncan I, Sullivan P, Lomas F. Sonography in the diagnosis of carpal tunnel syndrome. AJR Am J Roentgenol 1999;173:681—4.
[34] Lee D, van Holsbeeck MT, Janevski PK, et al. Diagnosis of carpal tunnel syndrome. Ultrasound versus electromyography. Radiol Clin North Am 1999;37:859—72.
[35] Sarría L, Cabada T, Cozcolluela R, Martínez-Berganza T, García S. Carpal tunnel syndrome: usefulness of sonography. Eur Radiol 2000;10:1920—5.
[36] El Miedany YM, Aty SA, Ashour S. Ultrasonography versus nerve conduction study in patients with carpal tunnel syndrome: substantive or complementary tests? Rheumatology (Oxford) 2004;43:887—95.
[37] Yesildag A, Kutluhan S, Sengul N, et al. The role of ultrasonographic measurements of the median nerve in the diagnosis of carpal tunnel syndrome. Clin Radiol 2004;59:910—5.
[38] Ziswiler HR, Reichenbach S, Vögelin E, et al. Diagnostic value of sonography in patients with suspected carpal tunnel syndrome: a prospective study. Arthritis Rheum 2005;52:304—11.
[39] Wiesler ER, Chloros GD, Cartwright MS, Smith BP, Rushing J, Walker FO. The use of diagnostic ultrasound in carpal tunnel syndrome. J Hand Surg [Am] 2006;31:726—32.

[40] Visser LH, Smidt MH, Lee ML. High-resolution sonography versus EMG in the diagnosis of carpal tunnel syndrome. J Neurol Neurosurg Psychiatry 2008;79:63—7.
[41] Moran L, Perez M, Esteban A, Bellon J, Arranz B, del Cerro M. Sonographic measurement of cross-sectional area of the median nerve in the diagnosis of carpal tunnel syndrome: correlation with nerve conduction studies. J Clin Ultrasound 2009;37:125—31.
[42] Klauser AS, Halpern EJ, De Zordo T, et al. Carpal tunnel syndrome assessment with US: value of additional cross-sectional area measurements of the median nerve in patients versus healthy volunteers. Radiology 2009;250:171—7.
[43] Hunderfund AN, Boon AJ, Mandrekar JN, Sorenson EJ. Sonography in carpal tunnel syndrome. Muscle Nerve 2011;44:485—91.
[44] Tajika T, Kobayashi T, Yamamoto A, Kaneko T, Takagishi K. Diagnostic utility of sonography and correlation between sonographic and clinical findings in patients with carpal tunnel syndrome. J Ultrasound Med 2013;32:1987—93.
[45] Hobson-Webb LD, Massey JM, Juel VC, et al. The ultrasonographic wrist-to- forearm median nerve area ratio in carpal tunnel syndrome. Clin Neurophysiol 2008;119:1353—7.
[46] Bayrack IK, Bayrak AO, Kale M, Turker H, Diren B. Bifid median nerve in patients with carpal tunnel syndrome. J ultrasound Med 2008;27:1129—36.
[47] Klauser AS, Halpern EJ, Faschingbauer R, et al. Bifid median nerve in carpal tunnel syndrome: assessment with US cross-sectional area measurement. Radiology 2011;259:808—15.
[48] Mondelli M, Filippou G, Gallo A, Frediani B. Diagnostic utility of ultrasonography versus nerve conduction studies in mild carpal tunnel syndrome. Arthritis Rheum 2008;59:357—66.
[49] Therimadasamy A, Pin Peng Y, Wilder-Smith EP. Carpal tunnel syndrome: median nerve enlargement restricted to the distal carpal tunnel. Muscle Nerve 2012;46:455—7.
[50] Paliwal PR, Therimadasamy AK, Chan YC, et al. Does measuring the median nerve at the carpal tunnel outlet improve ultrasound CTS diagnosis? J Neurol Sci 2014;339:47—51.
[51] Akcar N, Ozkan S, Mehmetoglu O, et al. Value of power Doppler and gray-scale US in the diagnosis of carpal tunnel syndrome: contribution of cross-sectional area just before the tunnel inlet as compared with the cross-sectional area at the tunnel. Korean J Radiol 2010;11:632—9.
[52] Joy V, Therimadasamy AK, Chan YC, Wilder-Smith EP. Combined Doppler and B-mode sonography in carpal tunnel syndrome. J Neurol Sci 2011;308:16—20.
[53] Dejaco C, Stradner M, Zauner D, et al. Ultrasound for diagnosis of carpal tunnel syndrome: comparison of different methods to determine median nerve volume and value of power Doppler sonography. Ann Rheum Dis 2013;72:1934—9.
[54] Nakamichi K, Tachibana S. Restricted motion of the median nerve in carpal tunnel syndrome. J Hand Surg [Br] 1995;20:460—4.
[55] Erel E, Dilley A, Greening J, Morris V, Cohen B, Lynn B. Longitudinal sliding of the median nerve in patients with carpal tunnel syndrome. J Hand Surg [Br] 2003;28:439—43.
[56] Fowler JR, Gaughan JP, Ilyas AM. The sensitivity and specificity of ultrasound for the diagnosis of carpal tunnel syndrome: a meta-analysis. Clin Orthop Relat Res 2011;469:1089—94.
[57] Ghasemi-Esfe AR, Khalilzadeh O, Vaziri-Bozorg SM, et al. Color and power Doppler US for diagnosing carpal tunnel syndrome and determining its severity: a quantitative image processing method. Radiology 2011;26:499—506.
[58] Klauser AS, Abd Ellah MM, Halpern EJ, et al. Sonographic cross-sectional area measurement in carpal tunnel syndrome patients: can delta and ratio calculations predict severity compared to nerve conduction studies? Eur Radiol 2015;25:2419—27.
[59] Touraine S, Wybier M, Sibileau E, Genah I, Petrover D, Parlier-Cuau C, et al. Non-traumatic calcifications/ossifications of the bone surface and soft tissues of the wrist, hand and fingers: a diagnostic approach. Diagn Interv Imaging 2014;95:1035—44.
[60] Żyluk A, Walaszek I, Szlosser Z. No correlation between sonographic and electrophysiological parameters in carpal tunnel syndrome. J Hand Surg Eur Vol 2014;39:161—6.
[61] El-Karabaty H, Hetzel A, Galla TJ, Horch RE, Lücking CH, Glocker FX. The effect of carpal tunnel release on median nerve flattening and nerve conduction. Electromyogr Clin Neurophysiol 2005;45:223—7.
[62] Abicalaf CA, De Barros N, Sernik RA, et al. Ultrasound evaluation of patients with carpal tunnel syndrome before and after endoscopic release of the transverse carpal ligament. Clin Radiol 2007;62:891—4.
[63] Mondelli M, Filippou G, Aretini A, Frediani B, Reale F. Ultrasonography before and after surgery in carpal tunnel syndrome and relationship with clinical and electrophysiological findings. A new outcome predictor? Scand J Rheumatol 2008;37:219—24.
[64] Smidt MH, Visser LH. Carpal tunnel syndrome: clinical and sonographic follow-up after surgery. Muscle Nerve 2008;38:987—91.
[65] Lee CH, Kim TK, Yoon ES, Dhong ES. Postoperative morphologic analysis of carpal tunnel syndrome using high-resolution ultrasonography. Ann Plast Surg 2005;54:143—6.
[66] Naranjo A, Ojeda S, Rúa-Figueroa I, et al. Limited value of ultrasound assessment in patients with poor outcome after carpal tunnel release surgery. Scand J Rheumatol 2010;39:409—12.
[67] Kim JY1, Yoon JS, Kim SJ, Won SJ, Jeong JS. Carpal tunnel syndrome: clinical, electrophysiological, and ultrasonographic ratio after surgery. Muscle Nerve 2012;45:183—8.
[68] O'Driscoll SW, Horii E, Carmichael SW, Morrey BF. The cubital tunnel and ulnar neuropathy. J Bone Joint Surg Br 1991;73B:613—7.
[69] Ozturk E, Sonmez G, Colak A, et al. Sonographic appearances of the normal ulnar nerve in the cubital tunnel. J Clin Ultrasound 2008;36:325—9.
[70] Filippou G, Mondelli M, Greco G, et al. Ulnar neuropathy at the elbow: how frequent is the idiopathic form? An ultrasonographic study in a cohort of patients. Clin Exp Rheumatol 2010;28:63—7.
[71] Van Den Berg PJ, Pompe SM, Beekman R, Visser LH. Sonographic incidence of ulnar nerve (sub)luxation and its associated clinical and electrodiagnostic characteristics. Muscle Nerve 2013;47:849—55.
[72] Nakano K, Murata K, Omokawa S, et al. Dynamic analysis of the ulnar nerve in the cubital tunnel using ultrasonography. J Shoulder Elbow Surg 2014;23:933—7.
[73] Mondelli M, Filippou G, Frediani B, Aretini A. Ultrasonography in ulnar neuropathy at the elbow: relationships to clinical and electrophysiological findings. Neurophysiol Clin 2008;38:217—26.
[74] Yoon JS, Walker FO, Cartwright MS. Ultrasonographic swelling ratio in the diagnosis of ulnar neuropathy at the elbow. Muscle Nerve 2008;38:1231—5.
[75] Volpe A, Rossato G, Bottanelli M, et al. Ultrasound evaluation of ulnar neuropathy at the elbow: correlation with electrophysiological studies. Rheumatology (Oxford) 2009;48:1098—101.
[76] Bayrak AO, Bayrak IK, Turker H, Elmali M, Nural MS. Ultrasonography in patients with ulnar neuropathy at the elbow: comparison of cross-sectional area and swelling ratio with electrophysiological severity. Muscle Nerve 2010;41:661—6.
[77] Gruber H, Glodny B, Peer S. The validity of ultrasonographic assessment in cubital tunnel syndrome: the value of a cubital-to-humeral nerve area ratio (CHR) combined with morphologic features. Ultrasound Med Biol 2010;36:376—82.
[78] Ayromlou H, Tarzamni MK, Daghighi MH, et al. Diagnostic value of ultrasonography and magnetic resonance imaging in ulnar neuropathy at the elbow. ISRN Neurol 2012;2012:491892.

[79] Pompe SM, Roy Beekman R. Which ultrasonographic measure has the upper hand in ulnar neuropathy at the elbow? Clinical Neurophysiology 2013;124:190—6.
[80] Kim JH, Won SJ, Rhee WI, Park HJ, Hong HM. Diagnostic cutoff value for ultrasonography in the ulnar neuropathy at the elbow. Ann Rehabil Med 2015;39:170—5.
[81] Omejec G, Zgur T, Podnar S. Diagnostic accuracy of ultrasonographic and nerve conduction studies in ulnar neuropathy at the elbow. Clin Neurophysiol 2015;126:1797—804.
[82] Zeiss J, Guilliam-Haidet L. MR demonstration of anomalous muscles about the volar aspect of the wrist and forearm. Clin Imaging 1996;20:219—21.
[83] Blum AG, Zabel JP, Kohlmann R, et al. Pathologic conditions of the hypothenar eminence: evaluation with multidetector CT and MR imaging. Radiographics 2006;26: 1021—44.
[84] Ferdinand B, Rosenberg ZS, Schweitzer ME, et al. MRI features of radial tunnel syndrome: initial experience. Radiology 2006;240:161—8.
[85] Khalil C, Budzik JF, Kermarrec E, Balbi V, Le Thuc V, Cotten A. Tractography of peripheral nerves and skeletal muscles. Eur J Radiol 2010;76:391—7.
[86] Miyamoto H, Halpern EJ, Kastlunger M, et al. Carpal tunnel syndrome: diagnosis by means of median nerve elasticity: improved diagnostic accuracy of US with sonoelastography. Radiology 2014;270:481—6.
[87] Moser T. Imagerie des traumatismes nerveux. In: Lhoste-Trouilloud A, editor. Le nerf périphérique. Sauramps Médical; 2015. p. 107—21.
[88] Kretschmer T, Antoniadis G, Braun V, et al. Evaluation of iatrogenic lesions in 722 surgically treated cases of peripheral nerve trauma. J Neurosurg 2001;94:905—12.
[89] Bodner G, Buchberger W, Schocke M, et al. Radial nerve palsy associated with humeral shaft fracture: evaluation with US: initial experience. Radiology 2001;219:811—6.
[90] Wavreille G, Clairemidi A, Sauvage A, et al. Lésions traumatiques des nerfs périphériques (plexus brachial exclu). EMC — Appar Locomoteur 2013;8:1—12.
[91] Umans H, Kessler J, de la Lama M, et al. Sonographic assessment of volar digital nerve injury in the context of penetrating trauma. AJR Am J Roentgenol 2010;194:1310—3.
[92] Soubeyrand M, Biau D, Jomaah N, et al. Penetrating volar injuries of the hand: diagnostic accuracy of US in depicting soft-tissue lesions. Radiology 2008;249:228—35.
[93] Tagliafico A, Pugliese F, Bianchi S, et al. High-resolution sonography of the palmar cutaneous branch of the median nerve. AJR Am J Roentgenol 2008;191:107—14.
[94] Baptista C, Iniesta A, Nguyen P, Legré R, Gay AM. Greffe de tissu adipeux autologue dans la prise en charge chirurgicale des cicatrices douloureuses: résultats préliminaires. Chir Main 2013;32:329—34.
[95] Atherton DD, Taherzadeh O, Facer P, Elliot D, Anand P. The potential role of nerve growth factor (NGF) in painful neuromas and the mechanism of pain relief by their relocation to muscle. J Hand Surg Br 2006;31:652—6.
[96] Dworkin RH, Handlin DS, Richlin DM, et al. Unraveling the effects of compensation, litigation, and employment on treatment response in chronic pain. Pain 1985;23:49—59.